Wavelength Dependence of the Primary Ozone Formation in High-Pressure O_2 and O_2/CO_2 Mixtures under Irradiation from 232 to 255 nm

Kazuko Sugimoto, Junichiro Otomo, and Seiichiro Koda*

Department of Chemical System Engineering, School of Engineering, The University of Tokyo, Hongo 7-3-1, Bunkyo-ku, Tokyo 113-8656, Japan

Received: February 7, 2002; In Final Form: October 31, 2002

Laser-induced reactions of O_2 to yield ozone (O_3) were investigated to estimate the quantum yield of primary odd-oxygen species production from photoabsorption by O_2 as a function of excitation laser wavelength from 232 to 255 nm. The experiments were carried out at 35 °C in pressurized O_2 (2.0 MPa) and O_2/CO_2 mixtures (9.6 MPa). The initial slope of O_3 formation versus irradiation time was used to obtain the quantum yield of the primary odd-oxygen species, minimizing possible catalytic O_3 production initiated by the subsequent photolysis of the product O_3. The quantum yield of the primary odd-oxygen species was shown to be almost 2 in pressurized O_2 at wavelengths shorter than 242 nm, i.e., the dissociation threshold of O_2. It was less than 2 in the O_2/CO_2 mixture and seemed to have a tendency to increase slightly in the shorter-wavelength region. At wavelengths between 242 and 252 nm, the quantum yield decreased monotonically with increasing laser wavelength both in O_2 and in O_2/CO_2 mixtures. It became almost 0 over the wavelength of 252 nm. These findings could not be explained by the contribution of the thermal energy of O_2 in the photodissociation process alone. Although thermal dissociation of O_2(A, A′, c) is not ruled out on the basis of the present experiments alone, the most likely mechanism is the thermal reaction of O_2(A, A′, c) to produce O + O_3, taking into account the temperature dependence experiments of Shi and Barker (*J. Geophys. Res.* **1992**, *97*, 13039).

Introduction

The photochemistry of the O_2 molecule in the ultraviolet wavelength region is of fundamental interest in physical chemistry and is also important in many other fields such as atmospheric chemistry and in application such as photooxidation.

In the field of atmospheric chemistry, the photoabsorption and subsequent reactions of O_2 are important because they can contribute to ozone (O_3) production. The abundance of O_2 in the atmosphere leads to light absorption of the same order of magnitude as that of O_3 in the strong ozone Hartley band (230−300 nm) region, and thus, the photochemistry of the excited O_2 should be very important. On the other hand, our study on the photoinduced partial oxidation of hydrocarbons in supercritical CO_2 suggests the formation of primary active oxygen species from O_2 when the mixture was irradiated at wavelengths longer than 242 nm.[1,2] Here, an understanding of O_2 photochemistry is also needed.

UV absorption of O_2 has long been known to be pressure-dependent[3−9]and was recently revisited by Fally et al.[10] at 2 cm^{-1} resolution. The pressure dependence is attributed to the interaction of O_2 with O_2 or foreign gases, which enhances the $A'^3\Delta_u \leftarrow X^3\Sigma_g^-$ transition of O_2. The collision-induced $A'^3\Delta_u \leftarrow X^3\Sigma_g^-$ transition named the Wulf band becomes exclusive under the high-pressure conditions adopted in the present experiments, although this absorption is weak and less important than the Herzberg I system (A ← X) in ambient atmosphere. The Wulf band does not have a sharp rotational structure and is constructed from diffuse structures in the wavelength region above 242 nm. It is not possible to excite a specific rotational level using monochromatic laser light.

The first dissociation limit of O_2 is located at 41 256.6 cm^{-1} (242.4 nm).[11] Slanger et al.[12] for the first time reported that a large density of O_3 is produced from unfocused 248-nm KrF excimer laser irradiation of 1000 Torr pure O_2. They noticed that there was some unknown initial mechanism to produce odd-oxygen species and observed the subsequent autocatalytic production of O_3. Once a small amount of O_3 is produced, it strongly absorbs the 248-nm light and dissociates partly to vibrationally excited O_2, which again absorbs the radiation to produce oxygen atoms. Thus, they made clear the existence of autocatalytic production mechanism of O_3 under 248-nm irradiation. Later, Shi and Barker[13] examined the same system kinetically at 200−1600 Torr and 298−370 K and concluded that the O_2(A, A′, and/or c) produced through the absorption of 248-nm light reacts with O_2(X) to generate odd-oxygen species as the primary products. In addition, Huestis et al.[14] reported the production of O atoms resulting through chemical reaction from the excitation of O_2 at 8−14 Torr. They recognized a good agreement between the rotational structures of the excitation spectrum of the O atom production and those of the $A^3\Sigma_u^- \leftarrow X^3\Sigma_g^-$ absorption measured by cavity ring-down spectroscopy from 11−0 to 8−0 bands of the $A^3\Sigma_u^+$ state. Copeland et al.[15] estimated the quantum yields for O atom production from the reaction of high-lying vibrational levels (v = 11−9) of the A state. On the other hand, Brown and Vaida[16] investigated the photolysis of O_2 dimer at wavelengths between 251 and 266 nm using the technique of supersonic expansion and concluded that the photoexcitation of O_2 dimer (X,A′ ← X,X) led to

* Corresponding author. Tel.: + 81-3-5841-7327. Fax: + 81-3-5841-7255. E-mail: koda@chemsys.t.u-tokyo.ac.jp.

10.1021/jp020367l CCC: $25.00
Published on Web 01/29/2003

decomposition into O and O_3. Their study showed that the closely approached pair of $O_2(A', A, \text{and/or } c^1\Sigma_u^-)$ and $O_2(X)$ could react to give $O + O_3$.

Thus, the photochemical behavior of pure O_2 system at 248 nm, as well as for several high vibrational levels of the A state, is now clarified. However, the dependence of the quantum yield of the primary odd-oxygen species (O, O_3) on the excitation wavelength is not yet established. To evaluate the contributions of absorption in the Herzberg bands and of their subsequent reactions with O_2 to produce odd-oxygen species in the atmosphere, knowledge of the quantum yield of the primary process as a function of the excitation wavelength is indispensable.

The same is true for the oxidation reactions in supercritical CO_2. In our laboratory, the property of supercritical CO_2 as the medium for the photoinduced partial oxidation of hydrocarbons was investigated.[1,2] The KrF-laser-induced oxidation of O_2/hydrocarbon mixtures in sub- and supercritical CO_2 was studied. It was found from the irradiation of high-pressure O_2/CO_2 mixtures that some odd-oxygen species were formed by the KrF laser irradiation, which were supposed to be responsible for the oxidation. The initial mechanism of the production of odd-oxygen species is considered to be very similar to that of the pure O_2 system. In the previous report we concluded that the main primary O_3 formation is due to the interaction of O_2(A, A′, and/or c) with CO_2.[17] However, the employed irradiation was limited to that produced by a KrF laser, and the behavior at different wavelengths is required.

In this paper, using a high-pressure photolysis cell, we measure the primary quantum yield of odd-oxygen species generated through the photoabsorption of O_2 followed by a prompt subsequent reaction in pressurized O_2 or O_2/CO_2, changing the wavelength of dye laser from 232 to 255 nm. The O_3 quantum yield measured in the initial stage just after the start of laser irradiation should correspond to the quantum yield of primary odd-oxygen species, because the primarily produced odd-oxygen species are expected to react with O_2 to yield O_3 promptly. The O_3 yield in later stages is strongly influenced by subsequent catalytic O_3 reactions, which are initiated by the photoabsorption of the O_3 produced. Because the fraction of photoabsorption by O_3 is smaller than that by O_2 under the higher total pressure because of the augmentation of absorption by O_2 with pressure, the high pressure of the present experiments has the merit that the contribution of catalytic O_3 formation is minimized. The production of the primary odd-oxygen species is thus much more precisely estimated in the present experiments compared to the previous literature reports.[13−15] We show that the quantum yield decreases with increasing wavelength. The mechanism of O_2 interaction in the Herzberg states with O_2 and CO_2 to produce odd-oxygen species is also discussed.

Experimental Section

The time evolution of O_3 was measured as a function of irradiation time using a pulsed dye laser at the desired wavelength for high-pressure O_2 and O_2/CO_2 mixtures. The high-pressure photolysis cell and procedures for the measurement of O_3 formation were almost the same as before[17] except for the irradiation laser. Briefly, a high-pressure cross-shaped optical cell made from stainless steel (SS 316) of 5.0 cm^3 inner volume that contained four sapphire windows of 8 mm thickness was employed. A magnetic rotor was used to stir the contents of the cell.

After the cell was evacuated, O_2 (Suzuki Shokan Co. Ltd., 99.7%, with impurities N_2, 0.2%; Ar, 0.05%; and H_2O, ca. 20 ppm) was first introduced into the cell up to 2.0 MPa (19.7 atm), i.e., 0.78 mol dm^{-3}, followed by the addition of CO_2 (Suzuki Shokan Co. Ltd., 99.7%), if necessary, up to the desired total pressure of 9.6 MPa (94.7 atm), i.e., 9.2 mol dm^{-3}. Then, the mixture was left for ca. 15 min to achieve a complete mixing with stirring. The mixture was irradiated at 35 °C by a frequency-doubled dye laser (Lambda Physik, SCANmate OPPO) pumped by a Nd:YAG laser (Spectra Physics, GCR170) with its wavelength in the range of 232−255 nm at the repetition rate of 10 Hz. The bandwidth of the laser wavelength was 0.15 cm^{-1}; the pulse width, 10 ns; a typical laser beam cross section, ca. 10 mm^2, and the pulse energy, 0.1−1.3 mJ $pulse^{-1}$. The path length for the laser irradiation was 3.3 cm. The laser intensity was monitored by a pyroelectric Joule meter (Gentec, ED-100A). During laser irradiation, the mixture in the cell was stirred by the magnetic rotor.

O_3 formation was monitored during the laser irradiation by UV absorption spectroscopy at 255 nm using a D_2 lamp as the light source and a 75-cm monochromator (Jobin-Yvon, HRS2) with 0.2-nm wavelength resolution. The absorption was measured perpendicular to the irradiation laser beam with an optical path length of 2.3 cm. A $CoSO_4$ aqueous solution (0.05 mol dm^{-3}, 1 cm thickness) was set between the D_2 lamp and the cell as an optical filter to cut the D_2 lamp light shorter than 210 nm.

In the O_3 concentration measurements, we evaluated inhomogeneities in the spatial distribution of O_3 concentration in the cell by using two different diameters of the spot of D_2 lamp light as before,[17] i.e., 4 and 8 mm. The spot size of the laser beam was fixed at 5 mm in the longitudinal direction and 3 mm in the lateral direction. Thus, all of the D_2 lamp light with the 4-mm diameter was within the laser beam path, and a part of D_2 light with the 8-mm diameter was out of the laser path. The measured concentration of O_3 was found not to be dependent on the spot size, which implies that the O_3 concentration distribution was effectively homogeneous. We also checked that, under the typical reaction conditions, the measured concentration of O_3 did not change appreciably after the interruption of irradiation with continued stirring. It was thus concluded that the observed O_3 concentration distribution was almost homogeneous in the cell as a result of the stirring.

Water can destroy O_3 through the HO_x cycle. We carried out an experiment with an additional 300 ppm H_2O under typical reaction conditions. The observed O_3 yield was found not to be affected by the presence of additional H_2O, and thus, we concluded that the effect of the impurity H_2O could be neglected. The mechanism in the presence of H_2O was also studied, as will be described in the Discussion section, which also supports the present conclusion.

Measurements of O_2 absorption in the mixtures were also carried out using the same experimental setup.

The density of the O_2/CO_2 mixture was estimated using the Peng−Robinson equation as before.[17,18] The critical temperature of the employed O_2/CO_2 mixture was estimated[19] to be 21.8 °C, which was lower than the experimental temperature, 35 °C.

Results

(1) Absorption Cross Section of O_2 in the UV Region. The absorption cross section of O_2 in the Herzberg band and continuum regions increases with increasing O_2 and/or foreign gas pressure,[3−9] and the absorptions are called Wulf bands and the Wulf continuum according to Fally et al.[10] The diffuse Wulf bands are the principal absorption under high pressures in the

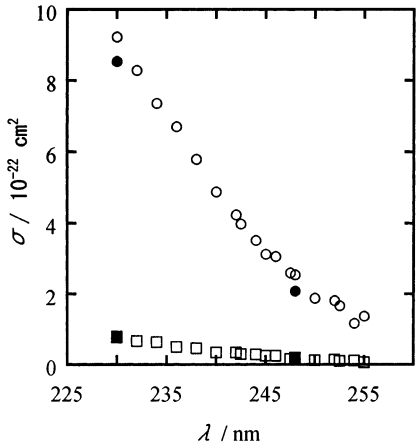

Figure 1. Absorption spectra of O_2 measured in a pressurized O_2 (2.0 MPa, 0.78 mol dm^{-3}, open squares) and O_2/CO_2 mixture (2.0 MPa, [O_2] 0.78 mol dm^{-3}, [CO_2] 9.22 mol dm^{-3}, open circles). The filled squares and circles are the estimated absorption cross sections in pressurized O_2 and O_2/CO_2 mixtures at 230 and 248 nm using the empirical equation in the literature.[8] The measurement was carried out at 35 °C.

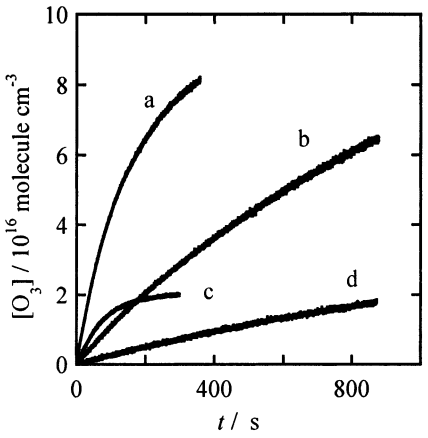

Figure 2. Typical time profiles of O_3 concentration under pulsed laser irradiation in pressurized O_2 and O_2/CO_2 mixtures. The laser wavelength and intensity were (a) 0.45 mJ pulse^{-1}, 10-Hz repetition, 236 nm, for the O_2/CO_2 mixture (9.6 MPa); (b) 0.55 mJ pulse^{-1}, 10-Hz repetition, 236 nm, for the pure O_2 (2.0 MPa); (c) 0.52 mJ pulse^{-1}, 10-Hz repetition, 244 nm, for the O_2/CO_2 mixture (9.6 MPa); and (d) 0.52 mJ pulse^{-1}, 10-Hz repetition, 245 nm, for the pure O_2 (2.0 MPa).

region longer than the dissociation limit, 242 nm. We measured the absorption cross section using a D_2 lamp as the light source under our experimental conditions, as shown in Figure 1. The obtained absorption cross sections are in good agreement with our previous values[8] at 230 and 248 nm within the error limit. The random error in the cross section was estimated to be ca. 10% in this measurement. Considering that the measured absorbance should be the same for the high-pressure diffuse bands between a D_2 lamp with a monochromator of 0.2-nm bandwidth and a pulsed laser with a resolution of 0.15 cm^{-1}, we used the absorption cross section in Figure 1 for the evaluation of the quantum yields.

(2) Time Profile of O_3 Formation and Estimation of O_3 Quantum Yield. The time profile of O_3 as a function of the irradiation time was measured using the same procedure as before, except that the irradiation laser was changed from the KrF excimer laser to the dye laser. The concentration of O_3 was calculated from the measured absorbance at 255 nm employing the O_3 absorption cross section of 1.16×10^{-17} cm^2 molecule^{-1} at 255 nm taken from literature.[20]

Typical time profiles of the O_3 concentration under dye laser irradiation in O_2 and in O_2/CO_2 mixtures at different wavelengths (236, 244, and/or 245 nm) are plotted against the irradiation time in Figure 2. The O_3 concentration increases monotonically with the irradiation time, and then, it gradually reaches a constant value. This feature is the same as obtained before with the KrF laser irradiation at 248 nm.[17] The saturation is mainly caused by the subsequent photolysis of O_3. It is expected that the primary O_3 quantum yield without any influence by subsequent catalytic O_3 reactions can be estimated from the initial time profile of the O_3 concentration.

First, we obtain the initial slope of the time profile, a

$$a = \mathrm{d}[\mathrm{O_3}]/\mathrm{d}t \quad \text{(extrapolated to } t = 0) \tag{1}$$

The absorbed amount of photons, N_{abs}, in the cell per unit time of irradiation is estimated as

$$N_{abs} = F\int_0^L I(l)\sigma_{O_2} n_{O_2}\,\mathrm{d}l \tag{2}$$

Here, the laser intensity, $I(l)$, at a certain cell position distant by l from the inner window surface for the laser inlet is

$$I(l) = AI_0 \exp(-\sigma_{O_2} n_{O_2} l) \tag{3}$$

Then

$$N_{abs} = AFI_0[1 - \exp(-\sigma_{O_2} n_{O_2} L)] \tag{4}$$

Here, I_0 and A are the intensity of the laser measured at the entrance of the cell and the transmittance of the sapphire window, respectively. F is the repetition rate of the laser pulses. L is the cell length. n_{O_2} is the number density of O_2, and σ_{O_2} is the absorption cross section of O_2 under the experimental conditions. Thus, the term $[1 - \exp(-\sigma_{O_2} n_{O_2} L)]$ corrects for the decrease in laser intensity along the cell length due to absorption by O_2. The laser intensity at the output window is about 92% of the incident laser intensity at 236 nm and 96% at 248 nm, in the high-pressure O_2. It is 35% at 236 nm and 67% at 248 nm in the O_2/CO_2 mixture. The absorption due to the O_3 formed can be neglected in the initial stage of the laser irradiation as will be described later. The quantum yield ϕ can be calculated by the following equation

$$\phi = aV/N_{abs} \tag{5}$$

where V is the volume of the cell. After a certain period of irradiation, O_3 accumulates, absorbs a certain fraction of the incident laser light, and also influences the relevant kinetics. The time necessary for O_3 to accumulate to a high enough concentration to absorb the same fraction of the irradiation laser as O_2 can be a certain measure of reaction progress. The above-defined times in the high-pressure O_2 are, for example, ca. 20 and 90 s for 240- and 245-nm laser irradiation, respectively. These times are long enough to allow for a reliable estimation of the initial slope by the extrapolation procedure.

It is worth noting that the present O_3 formation measurements correspond to the primary odd-oxygen species formation process from photoabsorption followed by a prompt subsequent reaction and are almost free of any contamination by the catalytic O_3 formation processes that were made clear by Slanger et al.[12] at 248 nm. This point will be discussed in detail in the Discussion section.

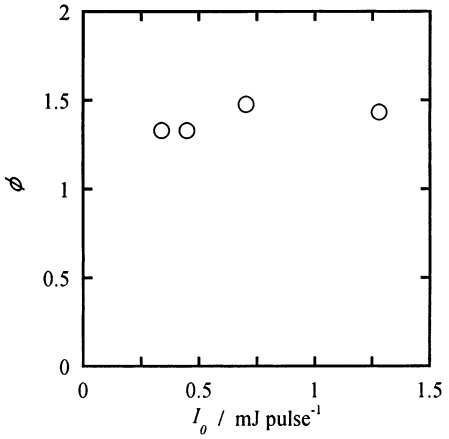

Figure 3. O_3 quantum yield plotted against the laser intensity in an O_2/CO_2 mixture. The measurement was carried out at 236 nm, 10 Hz, 0.34−1.28 mJ pulse^{-1}, and 35.0 °C for the mixture of total pressure, 9.6 MPa ([O_2], 0.78 mol dm^{-3}; [CO_2], 9.22 mol dm^{-3}).

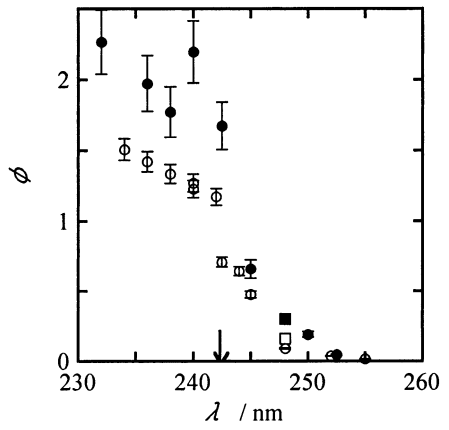

Figure 4. Wavelength dependence of the quantum yield of O_3 measured in a pressurized O_2 (2.0 MPa, 0.78 mol dm^{-3}, filled circles) and O_2/CO_2 mixture (2.0 MPa, [O_2] 0.78 mol dm^{-3}, [CO_2] 9.22 mol dm^{-3}, open circles). The filled square and open square at 248 nm are the quantum yields in pressurized O_2 and in an O_2/CO_2 mixture, respectively, reproduced from the previous study using a KrF excimer laser.[17] The error bars are the estimated random errors. The arrow indicates the dissociation threshold of O_2 at 242.4 nm.

(3) Dependence of the Quantum Yield on Laser Intensity. The dependence of the quantum yield on the intensity of the irradiation laser for the range 0.1−1.3 mJ pulse^{-1} was investigated at 236 nm for a typical O_2/CO_2 mixture, as shown in Figure 3. The estimated quantum yield was found to be independent of the laser intensity. Thus, the O_3 formation process is a one-photon process. A one-photon process was also established at 248 nm in our previous paper.[17]

(4) Dependence of the Quantum Yield on the Excitation Wavelength. The threshold for O_2 dissociation is located at 242.4 nm, and we are interested whether the wavelength dependence of the quantum yield changes through the threshold as well as with the absolute value itself. Thus, the quantum yield of O_3 formation was measured at about 10 different wavelengths from 232 to 255 nm. The results are plotted in Figure 4.

The random errors of the above O_3 quantum yields were estimated as shown below. They arise in measuring I_0 and calculating $[1 - \exp(-\sigma_{O_2} n_{O_2} L)]$. The fluctuation of the laser intensity I_0 was within 10%. We evaluated the errors in the latter term, $[1 - \exp(-\sigma_{O_2} n_{O_2} L)]$, taking into account the error of the absorption cross section, which was within 10% as described before, as well as the uncertainty in the density. For example, the errors in the term $[1 - \exp(-\sigma_{O_2} n_{O_2} L)]$ at 236 nm were evaluated to be 11 and 16% in O_2 and O_2/CO_2, respectively. Thus, the combined random errors of ϕ from the two terms, I_0 and $[1 - \exp(-\sigma_{O_2} n_{O_2} L)]$, are 11 and 13%, respectively for the O_2 and O_2/CO_2 mixture, provided that independent experiments were repeated 4 times. At other wavelengths, the errors are around the same or smaller than these values. The evaluated error ranges are indicated by bars at individual wavelengths in Figure 4.

The relationships in Figure 4 show distinctly different behaviors through ca. 242 nm, which corresponds to the dissociation threshold of O_2. In the shorter-wavelength region below 242 nm, the quantum yield appears to stay almost constant, although a slow increase with decreasing wavelength might exist as a real trend, particularly in O_2/CO_2 mixtures. The absolute value is close to 2 in pure O_2 and is smaller than 2 in the O_2/CO_2 mixtures. On the contrary, the quantum yield decreases rapidly with increasing wavelength in the region above 242 nm, and it is lower than the present detection limit at 255 nm in both pure O_2 and O_2/CO_2 mixtures. These findings suggest that the O_3 formation mechanism is different in the longer- and shorter-wavelength regions through 242 nm in both pressurized O_2 and O_2/CO_2.

Discussion

(1) Contribution of Subsequent Mechanisms to O_3 Formation. We are interested in the primary odd-oxygen formation quantum yield from photoexcited O_2 followed by a prompt subsequent reaction as a function of irradiation laser wavelength. Thus, we investigated the possibility of whether the observed *a* value contains contributions from any mechanisms other than the production of O_3 from photoexcited O_2.

First, the contribution of O_3 autocatalytic formation, which was extensively discussed by Slanger et al.[12] and Shi and Barker,[13] through the photodissociation of O_3 is taken into consideration. When the autocatalysis of O_3 is operative, the O_3 formation profile with laser irradiation time should have a concave shape in the middle stage and results in an S-shaped profile, considering the leveling-off due to the loss of odd-oxygen species by the recombination between odd-oxygen species in the final stage. We did not find any such tendency as shown in Figure 2, which evidences that the autocatalytic process does not contribute to any appreciable extent.

We will investigate more quantitatively the contribution that might exist even in the initial stages of laser irradiation. The vibrationally excited O_2, once it is generated by O_3 photolysis, plays a key role in the autocatalysis. However, it cannot survive the interval of laser pulses under the present high-pressure conditions. Thus, the contribution of autocatalytic O_3 formation to the total O_3 formation can be estimated by studying the reactions within a single laser pulse. The contribution can be measured by the ratio of the excess O_3 formation within a single laser pulse from the O_3 photolysis against the O_3 formation from the primary process derived by O_2 photoabsorption. The ratio R_{auto} is defined as

$$R_{auto} = (m - 1)\sigma_{O_3}[O_3]/(\phi\sigma_{O_2}[O_2]) \qquad (6)$$

where m is a multiplicative factor for evaluating the O_3 concentration resulting after the photolysis of O_3 caused by the autocatalytic process within a single laser pulse. ϕ is the primary quantum yield of odd-oxygen species, which is measured as the O_3 formation for photoexcited O_2 followed by a prompt subsequent reaction.

The multiplicative factor m can be estimated by solving the time evolution equation of following process during a single laser shot

$$O_3 + h\nu \rightarrow O(^3P) + O_2^{\ddagger} \quad (7)$$

$$\rightarrow O(^1D) + O_2 \quad (8)$$

$$O_2^{\ddagger} + h\nu \rightarrow 2O(^3P) \quad (9)$$

$$O(^3P) + O_2 + M \rightarrow O_3 + M \quad (10)$$

$$O(^1D) + M \rightarrow O(^3P) + M \quad (11)$$

$O_2^{\ddagger}$ represents vibrationally excited ground-state O_2. The branching ratio of reaction 7 is ca. 0.1 for 232−255-nm excitation.[21] We first estimate the multiplicative factor under the typical 248-nm irradiation for the 2 MPa O_2. When the pulse energy at 248 nm of a triangular pulse with a 10-ns fwhm is 1 mJ, the corresponding irradiation laser power at the maximum is 1.25×10^{15} photons cm^{-2} s^{-1}. Under typical reaction conditions at 248 nm, the O_3 concentration reaches 4×10^{15} molecules cm^{-3} at 50 s after the start of irradiation. Using the absorption cross section of O_3 as 1.07×10^{-17} cm^2,[20] the rate constant for reaction 10 as 5.6×10^{-34} cm^6 $molecule^{-2}$ s^{-1}, [22] and the absorption cross section of vibrationally excited $O_2^{\ddagger}$ as 2×10^{-18} cm^2 [23] (maximum value in the range $\upsilon = 12-20$) and assuming that reaction 11 proceeds instantaneously, the time profile of the O_3 decomposition and reproduction according to the reaction mechanism in eqs 7−11 was numerically calculated. At the end of the laser pulse, $m = 1.002$ has been obtained. Then, using σ_{O_2} as 1.96×10^{-23} cm^2 and assuming $\phi = 0.3$, the contribution ratio R_{auto} was evaluated to be 0.06. The R_{auto} value varies with the wavelength of the laser, the total pressure, and the quantum yield ϕ. Under typical conditions in pressurized O_2, the evaluated R_{auto} is 0.1 at 250 nm, 0.06 at 248 nm as described above, 0.03 at 245 nm, 0.008 at 240 nm, and 0.001 at 232 nm. In O_2/CO_2 mixtures, R_{auto} at any wavelength is smaller than the corresponding value in pressurized O_2. Thus, the contribution of the autocatalysis of O_3 is very small in both high-pressure O_2 and O_2/CO_2. Moreover, because we have indeed evaluated the quantum yield ϕ by extrapolating the time profile data to the initial stage after the pulse laser irradiation, the contribution is concluded to be negligible. We also used a similar procedure to study the probable contribution of the $O_2^{\ddagger}$ ($\upsilon > 25$) + O_2 reaction to the autocatalysis, because this reaction was once claimed to produce O + O_3.[24,25] We have concluded that the contribution is also negligible.

Second, the photolysis of O_2(a) and/or O_2(b) molecules that are produced in the system is also concluded to contribute to a negligible extent, because the lifetimes of such species are reported to be on the order of 10 ms,[26] so they do not survive the interval of the laser pulses.

Third, the contribution of H_2O reacting with $O(^1D)$ to yield two OH fragments and destroy ozone catalytically by the HO_x cycle was investigated, because a small amount of H_2O necessarily exists as an initial impurity in the reaction mixture. The reaction mechanism employed is

$$O(^1D) + H_2O \rightarrow 2OH \quad (12)$$

$$OH + O_3 \rightarrow HO_2 + O_2 \quad (13)$$

$$HO_2 + O_3 \rightarrow OH + 2O_2 \quad (14)$$

with appropriate radical−radical recombination reactions. The contribution of the above HO_x cycle with adequate rate constants[22] to the total O_3 formation rate was simulated to be smaller than 2% at an irradiation time of 60 s under typical reaction conditions with an additional 20 ppm H_2O. The negligible contribution of H_2O is consistent with the experiments with added H_2O described in the Experimental Section.

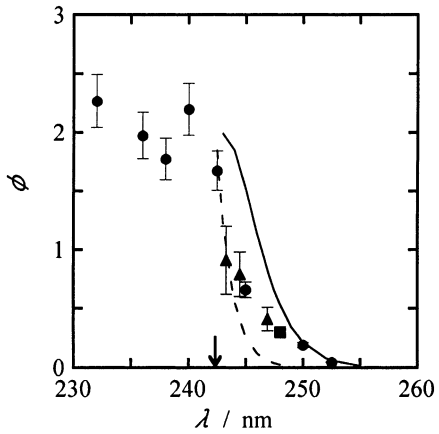

Figure 5. Comparison between the quantum yield of O_3 formation measured in pressurized O_2 (2.0 MPa, 0.78 mol dm^{-3}) and the simulation curves from the model. The experimental values are reproduced from Figure 4. The O atom quantum yields of Copeland et al.[15] are also shown by the filled triangles corresponding to the υ = 11, 10, and 9 vibrational levels of the A state. The broken line shows the fraction, f, of O_2 possessing enough energy to dissociate if the thermal rotational energy is taken into account, together with the light absorption at the given wavelength. The solid line shows the fraction, g, of $O_2(A,A',c)-O_2$ pairs possessing enough energy to dissociate if the thermal energy is taken into account, together with the light absorption at the given wavelength. The arrow indicates the dissociation threshold of O_2 at 242.4 nm.

Thus, we claim that the value a corresponds exclusively to the primary odd-oxygen formation from the photoexcited O_2 followed by a prompt subsequent reaction provided that the initially produced $O(^3P)$ is instantaneously converted to O_3.

(2) Primary Odd-Oxygen Formation Mechanism. *(2-1) Contribution of Thermal Rotational Excitation.* Despite the expectation that isolated O_2 cannot dissociate upon absorption of light with wavelengths longer than 242.4 nm, O_3 formation was eventually observed close to 255 nm. We first checked whether the thermal energy of O_2(X) can explain the production of O atoms at wavelengths longer than 242.4 nm. The population of vibrationally excited O_2 is negligibly small, because a vibrational quantum of O_2(X) is as large as 1500 cm^{-1}. Only the contribution of rotational energy, E_{rot}, is then taken into account. If the sum of the thermal rotational energy of ground-state O_2 and the absorbed photon energy is in excess of the dissociation energy, E_{th} (41 256.6 cm^{-1}), direct dissociation can occur provided that the restriction on rotational momentum can be neglected. The fraction, $f(E_{rot} \geq E_{th} - h\nu)$, of $O_2(X, J)$ can be calculated by the following equation

$$f(E_{rot} \geq E_{th} - h\nu) = \sum_{J,BJ(J+1) \geq E_{th} - h\nu}^{\infty} (2J+1) \exp[-BJ(J+1)] / \sum_{J} (2J+1) \exp[-BJ(J+1)] \quad (15)$$

Two times the fraction, $2f$, is considered to be the possible maximum quantum yield of O_3, which can be realized if the restriction due to the conservation of rotational angular momentum is mitigated in some way such as the collision with other molecules. The calculated $2f$ values are plotted against wavelength in Figure 5 and are compared with the experimental

O_3 quantum yields. It is concluded that the thermal rotational distribution is not enough to explain the O_3 formation in the range of wavelengths longer than the threshold wavelength.

(2-2) Photochemistry of O_2(A,A′,c)−O_2(X) in Pure O_2. The previous section shows that a certain interaction of photoexcited O_2 with other molecules is necessary for primary odd-oxygen species formation for wavelengths longer than the threshold. The mechanism proposed is shown below, following the work by Shi and Barker[13] and also our previous work[17] with 248-nm excitation.

$O_2(A'^3\Delta_u)$ is generated through O_2 absorption as a Wulf band under the present high-pressure conditions. Because $O_2(A'^3\Delta_u)$ is almost isoenergetic with $O_2(A^3\Sigma_u^+)$ and $O_2(c^1\Sigma_u^-)$, rapid internal conversion and/or intersystem crossing is expected to proceed among the three Herzberg states ($A^3\Sigma_u^+$, $A'^3\Delta_u$, and/or $c^1\Sigma_u^-$), and thus, it is not possible to distinguish one state from the other two states in the subsequent reactions. As already mentioned, Huestis et al.[14] and Copeland et al.[15] reported that the $A^3\Sigma_u^+$ state of O_2 reacts with O_2 to produce O atoms. O_2 molecules in the $A^3\Sigma_u^+$, $A'^3\Delta_u$, and/or $c^1\Sigma_u^-$ states will be described as O_2(A,A′,c).

The proposed mechanism for O_3 formation in the previous paper[17] is thus described by the following reactions

$$O_2(X) + h\nu \rightarrow O_2(A') \quad (16)$$

$$O_2(A') \rightleftarrows O_2(A,c) \quad (17)$$

$$O_2(A,A',c) + O_2(X) \rightarrow 2O(^3P) + O_2(X) \quad (18)$$

$$\rightarrow O(^3P) + O_3 \quad (19)$$

$$\rightarrow O_2(X) + O_2(X) \quad (20)$$

The model proposes that O_2(A,A′,c) collides with O_2(X) to dissociate into $2O(^3P)$, reacts to produce $O(^3P) + O_3$, and/or is electronically quenched. Under high-pressure O_2, $O(^3P)$ exclusively reacts with O_2 to yield O_3 by the reaction

$$O(^3P) + O_2(X) + M \rightarrow O_3 + M \quad (10)$$

Thus, the quantum yield of primary odd-oxygen species can be measured by that of O_3 in our high-pressure experiments, independent of whether the reaction is eq 18 or eq 19.

To explain the formation of O and/or O_3 in the longer-wavelength region, energy transfer during the interaction between O_2(A,A′,c) and O_2(X) is necessary, although we do not know whether the interaction time is very short or long enough to be imagined as formation of a complex. The sum of the heats of formation at 0 K of O and O_3 is calculated to be 392 kJ mol^{-1} from the 0 K enthalpies of formation,[27] which is less than the threshold energy of O_2 (41 256.6 cm^{-1} = 494 kJ mol^{-1}). If a certain long-lived complex is formed between O_2(A,A′,c) and O_2(X), the formation of O_3 might become energetically possible at relatively long wavelengths up to 305.1 nm from the above energetics.

We will check whether the thermal energy possessed by O_2(A,A′,c) + O_2(X) can explain, at least energetically, the formation of O and/or O_3 in the longer-wavelength region. The fraction $g(E_{thermal} \geq E_{th} - h\nu)$ of O_2(A,A′,c) + O_2(X) that possesses thermal energy greater than the difference between the threshold energy and the laser energy is calculated. Two times the g value is considered to correspond to the quantum yield of odd-oxygen species if the reaction is eq 18. The thermal energy $E_{thermal}$ is estimated as the sum of the rotational energies of O_2(A,A′,c), E_{rot1}, and O_2(X), E_{rot2}, and the relative translational energy, E_{trans}, between O_2(A,A′,c) and O_2(X), i.e.

$$E_{thermal} = E_{rot1} + E_{rot2} + E_{trans} \quad (21)$$

The fraction $g(E_{thermal} \geq E_{th} - h\nu)$ is calculated as

$$g(E_{thermal} \geq E_{th} - h\nu) = \sum_{J_1,J_2} p_{rot1} p_{rot2} p(E_{trans} \geq E_{th} - h\nu - E_{rot1} - E_{rot2}) \quad (22)$$

where p_{rot1} and p_{rot2} represent the probabilities that the rotational quantum number of O_2 is J_1 and J_2, respectively. $p(E_{trans} \geq E_{th} - h\nu - E_{rot1} - E_{rot2})$ representes the probability for the relative translational energy to exceed $E_{th} - h\nu - E_{rot1} - E_{rot2}$. The individual quantities are

$$p_{rot1} = (2J_1 + 1) \exp[-BJ_1(J_1 + 1)] / \sum_{J_1} (2J_1 + 1) \exp[-BJ_1(J_1 + 1)] \quad (23)$$

$$p_{rot2} = (2J_2 + 1) \exp[-BJ_2(J_2 + 1)] / \sum_{J_2} (2J_2 + 1) \exp[-BJ_2(J_2 + 1)] \quad (24)$$

$$p(E_{trans} \geq E_{th} - h\nu - E_{rot1} - E_{rot2}) = \int_{E_{th} - h\nu - E_{rot1} - E_{rot2}}^{\infty} \sqrt{E_{trans}} \exp(-E_{trans}/kT)\, dE_{trans} / \int_0^{\infty} \sqrt{E_{trans}} \exp(-E_{trans}/kT)\, dE_{trans} \quad (25)$$

Strictly speaking, the total thermal energy cannot be used for bond dissociation because of the restriction of angular momentum conservation. However, we are interested in the highest possible dissociation probability, and thus, all of the rotational and relative translational energy is assumed to be usable in O_2 bond dissociation. Here, we study the thermal dissociation of eq 18, and thus, the threshold energy E_{th} is set to the O_2 dissociation energy (41 256.6 cm^{-1} = 494 kJ mol^{-1}). The calculated quantum yield of primary O_3, i.e., $2g$, is plotted against the excitation wavelength in Figure 5. The $2g$ value is around the same as or even larger than the experimental quantum yield.

The above finding suggests as one possible mechanism that odd-oxygen species formation is caused by the thermal energy in the pair of O_2(A,A′,c) + O_2(X) within which efficient energy migration causes O−O bond dissociation. In other words, any complex formation between O_2(A,A′,c) and O_2(X) locating lower than the O−O bond dissociation threshold is not necessarily required to explain the formation of odd-oxygen species in the longer-wavelength region. However, it is important to note that the present finding never denies the possibility of the thermal reaction of O_2(A,A′,c) to produce O + O_3, as claimed by Shi and Barker.[13]

Shi and Barker measured the temperature dependence of the effective initiation cross section at 248 nm in pure O_2, which corresponds to the present quantum yield of odd-oxygen species when their value is divided by the O_2 absorption cross section.[13] Their effective cross section seems to stay rather independent

of the temperature (298−370 °C), and they stated that collisional dissociation

$$O_2(A,A',c) + M \rightarrow O(^3P) + O(^3P) + M \qquad (26)$$

is not adequate to explain their results, because the above mechanism requires a positive temperature dependence. When consider our study and Shi and Barker's results together, the most plausible mechanism to explain the production of odd-oxygen species in the longer-wavelength region is the thermal reaction of $O_2(A,A',c)$ to produce $O + O_3$, although the thermal dissociation of $O_2(A,A',c)$ is not ruled out on the basis of the present experiments alone.

When the wavelength of laser is shorter than 242.4 nm, the excited O_2 always has sufficient energy to dissociate without any interaction with other molecules. Experimental quantum yields are close to 2 at 232−242 nm, which supports the very prompt dissociation of the excited O_2. Any appreciable cage effect to restrict the O−O bond cleavage seems not to contribute under the present pure O_2 conditions.

(2-3) Comparison of the Quantum Yield with Other Works. Shi and Barker[13] reported the effective cross section of primary O_3 formation at 248 nm. According to their reported cross section and the estimated absorption cross section of O_2 at their experimental pressure, we have estimated the quantum yield to be 0.24−0.30 in pure O_2 at 0.03−0.21 MPa. This value is in reasonable agreement with the present 2.0 MPa result, which is 0.19 at 250 nm.

Copeland et al.[15] reported the O atom production quantum yield for $v = 11$, 10, and 9 levels from the reaction of vibrationally excited A-state O_2 and ground-state O_2. Unfortunately, the experimental temperature was not reported but was guessed to be room temperature. Their values are plotted in Figure 5, at the wavelength corresponding to the vibronic energy of the A(v) state. If the reaction between $O_2(A)$ and $O_2(X)$ produces two atoms of oxygen through O−O bond dissociation as described by eq 18, their data can be compared directly with our quantum yield of the primary odd-oxygen species. This is because, in the experiments by Copeland et al., the pressure was so low that the atomic oxygen produced should stay as atomic oxygen all through the detection time. As seen in Figure 5, the data of Copeland et al. seem to exhibit a similar dependence of the quantum yield against the wavelength, when compared with the present experiments. On the other hand, if the reaction studied by Copeland et al. was eq 19, their O-atom yield must be multiplied by 2 for comparison with our primary quantum yield of odd-oxygen species. In this case, their data are larger than our data. It is plausible that the $O_2(A,A',c) + O_2(X)$ reaction produces 2 $O(^3P)$, utilizing the thermal energy, both in the Copeland et al. experiments and in the present experiments. However, it is also possible that the main reaction is eq 19 within the experimental uncertainty of the two experiments.

(2-4) O_3 Formation Mechanism in O_2/CO_2 Mixtures. The O_3 formation quantum yield in O_2/CO_2 mixtures decreased with increasing excitation laser wavelength. Indeed, the trends found in the wavelength dependence of the O_3 formation quantum yield were similar between the O_2 and O_2/CO_2, although the absolute values of the quantum yield in the mixture were smaller than those in pure O_2. In the present experiments, the molar ratio of O_2 to CO_2 in the adopted mixture was 0.78/9.22. Admitting that the absorption augmentation[8] and also the collisional quenching rate constant[28] are not so different between O_2 and CO_2, the O_3 formation quantum yield is considered

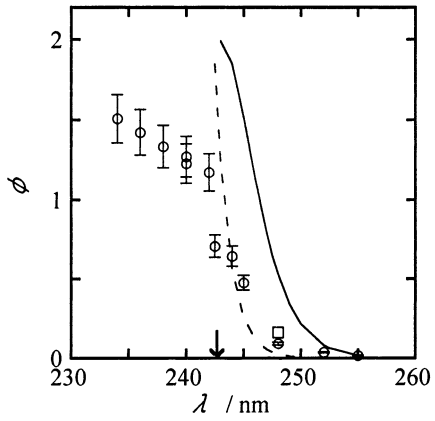

Figure 6. Comparison between the quantum yield of O_3 formation measured in O_2/CO_2 mixture (2.0 MPa, $[O_2]$ 0.78 mol dm^{-3}, $[CO_2]$ 9.22 mol dm^{-3}) and the simulation curves from the model. The experimental values are reproduced from Figure 4. The broken line shows the fraction, *f*, of O_2 possessing enough energy to dissociate if the thermal rotational energy is taken into account, together with the light absorption at the given wavelength. The solid line shows the fraction, *g*, of $O_2(A,A',c)-CO_2$ pairs possessing enough energy to dissociate if the thermal energy is taken into account, together with the light absorption at the given wavelength. The arrow indicates the dissociation threshold of O_2 at 242.4 nm.

to be exclusively controlled by $O_2(A,A',c)-CO_2$ interactions, and the contribution of $O_2(A,A',c)-O_2$ interactions can be neglected.

In O_2/CO_2 mixtures, an analogous mechanism is proposed as shown below

$$O_2(X) + h\nu \rightarrow O_2(A') \qquad (16)$$

$$O_2(A') \rightleftarrows O_2(A,c) \qquad (17)$$

$$O_2(A,A',c) + CO_2 \rightarrow 2O(^3P) + CO_2 \qquad (27)$$

$$\rightarrow \text{products } (O_3 + CO \text{ or } O + CO_3) \qquad (28)$$

$$\rightarrow O_2(X) + CO_2 \qquad (29)$$

$$O(^3P) + O_2(X) + M \rightarrow O_3 + M \qquad (10)$$

Reaction 27 is the dissociation of the O−O bond through the collision of CO_2, and reaction 28 corresponds to oxygen atom migration in the CO_2-O_2 pair. The products were not identified experimentally.

We have calculated the fraction, $g(E_{thermal} \geq E_{th} - h\nu)$, of O_2-$(A,A',c) + CO_2$ that possesses the thermal energy larger than the difference between the threshold energy and the laser energy, just as in pure O_2. The 2*g* values are plotted in Figure 6. The 2*f* values for the rotation of O_2 are also plotted. It is again clear that the thermal rotational energy of O_2 alone is not sufficient to explain the formation of odd-oxygen species at longer wavelength. However, O−O bond dissociation under irradiation at wavelengths longer than the dissociation threshold is possible with the thermal energy contained in the pair $O_2(A,A',c) + CO_2$.

(2−5) O_3 Formation Mechanism in O_2/CO_2 Mixtures at Wavelengths Shorter than 242.4 nm. Another important issue in O_3 formation in O_2/CO_2 mixtures is that experimental value of ϕ is less than 2 even at $\lambda < 242.4$ nm. If only the photodissociation of O_2 (eq 27) is contributing, the quantum yield of O_3 should be 2. Thus, a quantum yield of less than 2 implies the following two possibilities: reactions such as reaction 28 mainly contribute to O_3 formation or a certain cage

effect that lowers the photodissociation probability is effective. The sum of heat of formation for O_3 and CO (425 kJ mol^{-1})[27] is smaller than the sum of the heats of formation of O + O + CO_2 (494 kJ mol^{-1}).[11] The heat of formation of CO_3 is not established. At any rate, a photoinduced reaction to produce odd-oxygen species might be possible at least energetically up to 281.6 nm.

On the other hand, a certain cage effect that lowers the dissociation probability of O_2 might not be negligible in high-pressure O_2/CO_2 mixtures. Troe and co-workers[29,30] studied I_2 photodissociation in sub- and supercritical fluids. From their results, the photolysis quantum yield of I_2 is ca. 0.5 in 6 mol dm^{-3} CO_2. In our O_2/CO_2 system (0.78 mol dm^{-3} O_2, 9.22 mol dm^{-3} CO_2), a similar effect is suggested to occur.

At present, however, we cannot estimate the contribution of the two possible mechanisms quantitatively; one is the reaction of $O_2 + CO_2$ to form $O_3 + CO$ or $O + CO_3$, and the other is the cage effect. Identification of products, measurements of the dependence of the quantum yield on temperature and pressure, and experiments with other third gases are desirable.

(3) Atmospheric Implications. The atmospheric implications of excited O_2 in the UV region has been discussed by previous researchers,[13] and they stated that $O_2(A) + O_2$ reactions following O_2 absorption contribute up to ca. 6% of total odd-oxygen production at a height of around 50 km. Because they assumed that the Herzberg band states in the UV region dissociate independent of the wavelength, their evaluation is suspected to be somewhat larger than the real contribution. The present quantum yields as a function of wavelength indicate that more accurate estimations of the relevance of absorption of solar light by O_2 under various conditions are necessary.

(4) Concluding Remarks. The wavelength dependence of the quantum yield of primary odd-oxygen species was examined as a function of the excitation wavelength. The quantum yield showed different behaviors through ca. 242 nm, which corresponds to the dissociation threshold of O_2.

At wavelengths between 242 and 252 nm, the quantum yield decreased monotonically with increasing laser wavelength in both O_2 and O_2/CO_2 mixtures. It became almost 0 at wavelengths greater than 252 nm. These findings could not be explained by the contribution of the thermal energy of O_2 in the photodissociation process alone. One possible mechanism that is consistent with the present finding is the thermal dissociation of O_2(A,A′,c) with the aid of thermal energy transfer from O_2(X) or CO_2. However, it is not consistent with the temperature dependence measured by Shi and Barker. Thermal reaction of O_2(A,A′,c) with O_2 (or CO_2) to produce $O + O_3$ might be the most likely mechanism, which is strongly supported by the experiment by Shi and Barker and also does not contradict with the present results.

When the excitation wavelength was shorter than 242 nm, the primary quantum yield was almost independent of the wavelength. In pressurized O_2 (2.0 MPa), the quantum yield was ca. 2, and in pressurized O_2/CO_2 mixtures (9.6 MPa), it was less than 2 even for the range of wavelengths below 242 nm. It has a tendency to increase with decreasing wavelength. Solvent cage effect might be operative to some extent in pressurized O_2/CO_2 mixtures (9.6 MPa).

The present results would be useful for atmospheric modeling. The production of odd-oxygen species at wavelengths longer than 242.4 nm with the determined quantum yield in O_2 where no appreciable cage effect is expected should be incorporated in the calculation of the O_3 budget. Another important application is related to the issue of the initiation of oxidation in high-pressure CO_2 fluids. It has been evidenced that oxidation in hydrocarbon/O_2/CO_2 mixtures can be initiated by the primary photoinduced production of odd-oxygen species under UV irradiation.

Acknowledgment. The present work was supported by a Grant-in-Aid for Scientific Research (A) from the Ministry of Education, Science and Culture of Japan (No. 12305051), which is greatly appreciated.

References and Notes

(1) Koda, S.; Oshima, Y.; Otomo, J.; Ebukuro, T. *Process Technol. Proc.* **1996**, *12*, 97.
(2) Koda, S.; Ebukuro, T.; Otomo, J.; Tsuruno, T.; Oshima, Y. *J. Photochem. Photobiol. A: Chem.* **1998**, *115*, 7.
(3) Shardanand; Prasad Rao, A. D. *J. Quant. Spectrosc. Radiat. Transfer* **1977**, *17*, 433.
(4) Shardanand *J. Quant. Spectrosc. Radiat. Transfer* **1977**, *18*, 525.
(5) Amoruso, A.; Crescentini, L. *J. Quant. Spectrosc. Radiat. Transfer* **1995**, *53*, 457.
(6) Johnston, H. S.; Paige, M.; Yao, F. *J. Geophys. Res.* **1984**, *89*, 11661.
(7) Blake, A. J.; McCoy, D. G. *J. Quant. Spectrosc. Radiat. Transfer* **1987**, *38*, 113.
(8) Oshima, Y.; Okamoto, Y.; Koda, S. *J. Phys. Chem.* **1995**, *99*, 11830.
(9) Bernath, P.; Carleer, M.; Fally, S.; Jenouvrier, A.; Vandaele, A. C.; Hermans, C.; Mérienne, M.-F.; Colin, R. *Chem. Phys. Lett.* **1998**, *297*, 293.
(10) Fally, S.; Vandaele, A. C.; Carleer, M.; Hermans, C.; Jenouvrier, A.; Mérienne, M.-F.; Coquart, B.; Colin, R. *J. Mol. Spectrosc.* **2000**, *204*, 10.
(11) Pernot, C.; Durup, J.; Ozenne, J.-B.; Beswick, J. A.; Cosby, P. C.; Moseley, J. T. *J. Chem. Phys.* **1979**, *71*, 2387.
(12) Slanger, T. G.; Jusinski, L. E.; Black, G.; Gadd, G. E. *Science* **1988**, *241*, 945.
(13) Shi, J.; Barker, J. R. *J. Geophys. Res.* **1992**, *97*, 13039.
(14) Huestis, D. L.; Copeland, R. A.; Knutsen, K.; Slanger, T. G. *Can. J. Phys*. **1994**, *72*, 1109.
(15) Copeland, R. A.; Knutsen, K.; Slanger, T. G. In *Proceedings of the International Conference on Lasers '93*; Society for Optical and Quantum Electronics: McLean, VA, 1994; p 318.
(16) Brown, L.; Vaida, V. *J. Phys. Chem*. **1996**, *100*, 7849.
(17) Otomo, J.; Oshima, Y.; Takami, A.; Koda, S. *J. Phys. Chem. A* **2000**, *104*, 3332.
(18) Peng, D. Y.; Robinson, D. B. *AIChE J*. **1977**, *23*, 137.
(19) Liu, Z.-Y. *AIChE J*. **1998**, *44*, 1709.
(20) Molina, L. T.; Molina, M. J. *J. Geophys. Res.* **1986**, *91*, 14501.
(21) Cooper, L. A.; Neill, P. J.; Wiesenfeld, J. R. *J. Geophys. Res.* **1993**, *98*, 12795.
(22) DeMore, W. B.; Sander, S. P.; Howard, C. J.; Ravishankara, A. R.; Golden, D. M.; Kolb, C. E.; Hampson, R. F.; Kurylo, M. J.; Molina, M. J. *Chemical Kinetics and Photochemical Data for Use in Stratospheric Modeling*; Evaluation No. 12, JPL Publication 97-4; Jet Propulsion Laboratory: Pasadena, CA, 1997.
(23) Saxon, R. P.; Slanger, T. G. *J. Geophys. Res*. **1991**, *96*, 17291.
(24) Rogaski, C. A.; Price, J. M.; Mack, J. A.; Wodtke, A. M. *Geophys. Res. Lett*. **1993**, *20*, 2885.
(25) Miller, R. L.; Suits, A. G..; Houston, P. L.; Toumi, R.; Mack, J. A.; Wodtke, A. M. *Science* **1994**, *265*, 1831.
(26) Worrall, D. R.; Abdel-Shafi, A. A.; Wilkinson, F. *J. Phys. Chem. A* **2001**, *105*, 1270.
(27) Chase, M. W., Jr. *NIST−JANAF Thermochemical Tables*, 4th ed.; J. Phys. Chem. Ref. Data Monograph No. 9; Joint publication of the American Chemical Society and the American Institute of Physics for the National Institute of Standards and Technology: New York, 1988; Parts I and II.
(28) Knutsen, K.; Dyer, M. J.; Copeland, R. A. *J. Chem. Phys.* **1994**, *101*, 7415.
(29) Otto, B.; Schroeder, J.; Troe, J. *J. Chem. Phys.* **1984**, *81*, 202.
(30) Troe, J. *J. Phys. Chem.* **1986**, *90*, 357.